Mechanism of the Yb–Er energy transfer in fluorozirconate glass

L. D. da Vila, L. Gomes, L. V. G. Tarelho, S. J. L. Ribeiro, and Y. Messadeq

Citation: Journal of Applied Physics **93**, 3873 (2003); doi: 10.1063/1.1555679
View online: http://dx.doi.org/10.1063/1.1555679
View Table of Contents: http://scitation.aip.org/content/aip/journal/jap/93/7?ver=pdfcov
Published by the AIP Publishing

Mechanism of the Yb–Er energy transfer in fluorozirconate glass

L. D. da Vila, L. Gomes,[a] and L. V. G. Tarelho
Centro de Lasers e Aplicações, IPEN-SP, Travessa R 400, Cidade Universitária, CEP 05508-900, São Paulo, Brazil

S. J. L. Ribeiro and Y. Messadeq
Laboratório de Materiais Fotônicos, Instituto de Química de Araraquara, UNESP, São Paulo, Brazil

(Received 4 October 2002; accepted 3 January 2003)

The mechanism of the $Yb^{3+} \rightarrow Er^{3+}$ energy transfer as a function of the donor and the acceptor concentration was investigated in $Yb^{3+}-Er^{3+}$ codoped fluorozirconate glass. The luminescence decay curves were measured and analyzed by monitoring the $Er^{3+}(^4I_{11/2})$ fluorescence induced by the $Yb^{3+}(^2F_{5/2})$ excitation. The energy transfer microparameters were determined and used to estimate the Yb–Er transfer rate of an energy transfer process assisted by excitation migration among donors state (diffusion model). The experimental transfer rates were determined from the best fitting of the acceptor luminescence decay obtained using a theoretical approach analog to that one used in the Inokuti–Hirayama model for the donor luminescence decay. The obtained values of transfer parameter gamma $[\gamma(\text{exp})]$ were always higher than that predicted by the Inokuti–Hirayama model. Also, the experimental transfer rate, $\gamma^2(\text{exp})$, was observed to be higher than the transfer rate predicted by the migration model. Assuming a random distribution among excited donors at the initial time $(t=0)$ and that a fast excitation migration, which occurs in a very short time $(t \ll \gamma^{-2})$, reducing the mean distance between donor (excited) and acceptor, all the observed results could be explained. © *2003 American Institute of Physics.* [DOI: 10.1063/1.1555679]

I. INTRODUCTION

Fluoride glasses are well known by their high transparency in the mid-infrared,[1] low phonon energy,[2–4] and low attenuation of radiation near 1.5 μm in comparison with commonly used silica, silicate, and phosphate glasses.[5] Particularly, fluorozirconate glasses as ZBLAN ($ZrF_4-BaF_2-LaF_3-AlF_3-NaF$) have unique optical properties in the infrared region[6] and wide spectral range of optical transparency. These favorable physical properties make them excellent material for optical systems design[7] when doped with triply ionized rare earth ions. Particularly, the $^4I_{13/2} \rightarrow {}^4I_{15/2}$ luminescence of Er^{3+} at 1.5 μm has been extensively studied for the purpose of developing a light amplifier for telecommunication devices made of fiber glasses.[8–10] Also, the $^4I_{11/2} \rightarrow {}^4I_{13/2}$ emission of erbium at 2.7 μm in fluoride glasses constitutes a very promising system to construct all solid state lasers emitting near 3 μm to be applied as surgical instruments.[11–14] However, the energy level scheme of Er^{3+} does not favor the optical amplification at 1.5 μm because the three levels system involved. On the other hand, ytterbium ions exhibit a higher absorption cross section and a broad absorption band in this spectral region in comparison with erbium. These spectroscopic characteristics of ytterbium and the large spectral overlap between Yb^{3+} emission $(^2F_{5/2} \rightarrow {}^2F_{7/2})$ and the Er^{3+} absorption $(^4I_{15/2} \rightarrow {}^4I_{11/2})$ results in an efficient Yb→Er energy transfer (ET) in Yb–Er codoped materials.[15]

The aim of this article is to report the results of our investigation on the mechanism involved in the Yb→Er energy transfer (ET) observed in Yb:Er:ZBLAN glasses, using several combinations of Yb^{3+} (donor) and Er^{3+} (acceptor) concentrations. In this sense the donor–donor, donor–acceptor, and acceptor–donor energy-transfer constants (C_{DD}, C_{DA}, and C_{AD}) were determined and applied to estimate the expected transfer rate for the case of an energy transfer assisted by a diffusion model. However, the experimental transfer rates and the efficiencies were determined from the best fitting of a theoretical expression derived for the acceptor luminescence decay based on the Inokuti–Hirayama[16] approach. As a general result, the experimental energy transfer rates are higher than those predicted by the diffusion model. Based on this observation, a model including direct donor to acceptor energy transfer following the fast excitation diffusion among donors ($t \ll \gamma^{-2}$) was proposed.

II. EXPERIMENT

A. Glass preparation

Ytterbium and erbium fluorides were used, respectively, as codopant and dopant starting materials. They were prepared by fluorination of the respective ultrapure oxides (99.999%) from Alfa Aesar. Other chemicals employed to prepare ZBLAN glasses were the grade reagents (>99.9%) fluorides: ZrF_4 (Fluortran), BaF_2 (Alfa Aesar), LaF_3 (reactron, Alfa Aesar), AlF_3, and NaF (Fluortran). Three series of Yb:Er:ZBLAN glasses were prepared with the following compositions, where x and y are given in mol %:

(i) $(99-x)(53ZrF_4 \cdot 20BaF_2 \cdot 4LaF_3 \cdot 3AlF_3 \cdot 20NaF) \cdot x YbF_3 \cdot 1ErF_3$ ($x=0.2$, 0.3, 0.5, 1.0, 3.0, 4.5, and 6).

(ii) $(94-y)(53ZrF_4 \cdot 20BaF_2 \cdot 4LaF_3 \cdot 3AlF_3 \cdot 20NaF)$

[a]Electronic mail: lgomes@net.ipen.br

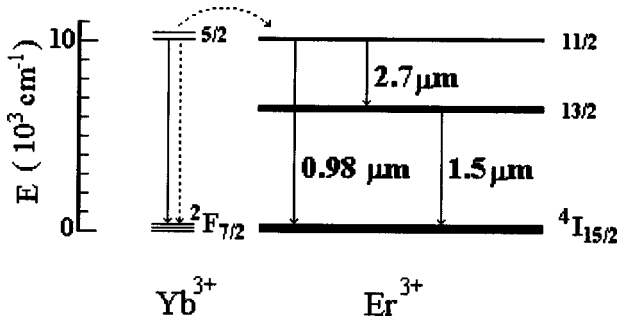

FIG. 1. A simplified energy level diagram of Yb:Er:ZBLAN which exhibits the Yb→Er energy transfer and the radiative transitions involved. Dashed and solid lines indicate the respective nonradiative and radiative processes.

$\cdot 6YbF_3 \cdot yErF_3$ ($y=1$, 2, 3, 4, and 5).

(iii) $(99-x)(53ZrF_4 \cdot 20BaF_2 \cdot 4LaF_3 \cdot 3AlF_3 \cdot 20NaF)$
$\cdot 1YbF_3 \cdot yErF_3$ ($y=1$, 2, 3, 4, and 5).

Yb:Er:ZBLAN glasses of 5 g were produced by melting processing at 750–800 °C for 2 h in a tubular furnace. A platinum crucible in the form of a tube was used as a sample container. After fusion, the melt was poured into a stainless steel mold preheated to 260 °C to form a rectangular glass. Annealing at 260 °C for 2 h was performed after casting. Finally, the samples were polished using isopropyl alcohol as a lubricanting agent.

B. Spectroscopic measurements

A time resolved luminescence spectroscopy was employed to measure the donor and acceptor luminescence decays induced by resonant laser excitations to determine the mechanism involved in $Yb^{3+}(^2F_{5/2}) \rightarrow Er^{3+}(^4I_{11/2})$ energy transfer. The lifetimes of excited Yb^{3+} and Er^{3+} were measured using a pulsed laser excitation (4 ns) from a tunable optical parametric oscillator pumped by the second harmonic of a *Q*-switched Nd-YAG laser from Quantel. Laser excitation at 0.93 μm was used to excite the $^2F_{5/2}$ state of Yb^{3+} and laser excitations at 0.98 and 1.5 μm were used to excite the $^4I_{11/2}$ and $^4I_{13/2}$ states of Er^{3+}, respectively. The time-dependent luminescence of the donor and the activator were detected by a InSb (77 K) infrared detector (Judson model J10D) with a fast preamplifier (response time of 0.5 μs) and analyzed using a signal-processing box-car averager (PAR 4402) or a digital 200 MHz oscilloscope from Tektronix (TDS 410). All the fluorescence decay times were measured at 300 K.

III. RESULTS

A. Determination of the energy transfer microparameters

A schematic energy level diagram representing the Yb→Er energy transfer, as well the 0.98, 1.5, and 2.7 μm Er^{3+} emissions involved, is exhibited in Fig. 1. The lifetime of the $^2F_{5/2}$ state of Yb^{3+} was measured for single- and double-doped ZBLAN glasses. Figure 2 shows the luminescence decay and best fittings. The single doped samples exhibited an exponential luminescence time decay with a lifetime of 2.7 ms. A weak residual luminescence of Yb^{3+} ions

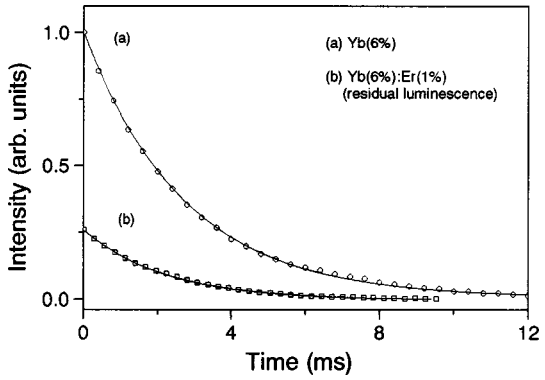

FIG. 2. Fluorescence decay of the $^2F_{5/2}$ level of Yb^{3+} in ZBLAN measured at 0.93 μm for two samples: single doped with Yb=6 mol % [curve (a)] and double-doped with [Yb]=6 mol % and [Er]=1 mol % [curve (b)]. The fluorescence was excited using a laser pulse of 7 mJ (4 ns, 10 Hz) at 0.920 μm.

was observed in double-doped samples with a Yb^{3+} lifetime of ~2.1 ms. This residual luminescence of Yb^{3+} ions was estimated to be produced by ~30% of the initial excited Yb^{3+} ions remaining in the $^2F_{5/2}$ state due to the $Er(^4I_{11/2}) \rightarrow Yb(^2F_{5/2})$ backtransfer process. This effect on Yb^{3+} luminescence is consistent with our backtransfer ratio estimate of 0.67 (see Table I) and is close to the previous ratio (0.75) found in the literature.[17]

The microparameters (C_{DD}, C_{DA}, and C_{AD}) involved in the energy transfer from the first and the second excited states of donors (D) to the acceptors (A) were calculated using

$$C_{DA}=\frac{R_{DA}^6}{\tau_D}, \tag{1}$$

$$C_{DD}=\frac{R_{DD}^6}{\tau_D}, \tag{2}$$

$$C_{AD}=\frac{R_{AD}^6}{\tau_A}, \tag{3}$$

where τ_D and τ_A are the total lifetime of the donor and acceptor state, respectively, measured in single doped samples. The critical radii R_{DD}, R_{DA}, and R_{AD} were calculated using the overlap integral method based on the calculation of the emission (donor) and the absorption (acceptor) cross-section superposition. The following expression were used:

TABLE I. The microparameters calculated for the nonradiative energy transfer from the first excited state of Yb^{3+} to the second excited state of Er^{3+} ions in ZBLAN glasses. C_{DD}, C_{DA}, and C_{AD} constants were obtained by using the method of the overlap integral for resonant energy transfers. R_C is the critical radius of the interaction.

Energy transfer	Transfer constant ($cm^6\ s^{-1}$)	R_c (Å)
$Yb(^2F_{5/2}) \rightarrow Yb(^2F_{5/2})$	$C_{DD}=(6.77\pm0.94)\times10^{-39}$	16.2
$Yb(^2F_{5/2}) \rightarrow Er(^4I_{11/2})$	$C_{DA}=(1.76\pm0.24)\times10^{-39}$	13.0
$Er(^4I_{11/2}) \rightarrow Yb(^2F_{5/2})$ (backtransfer)	$C_{AD}=(1.18\pm0.16)\times10^{-39}$	14.3

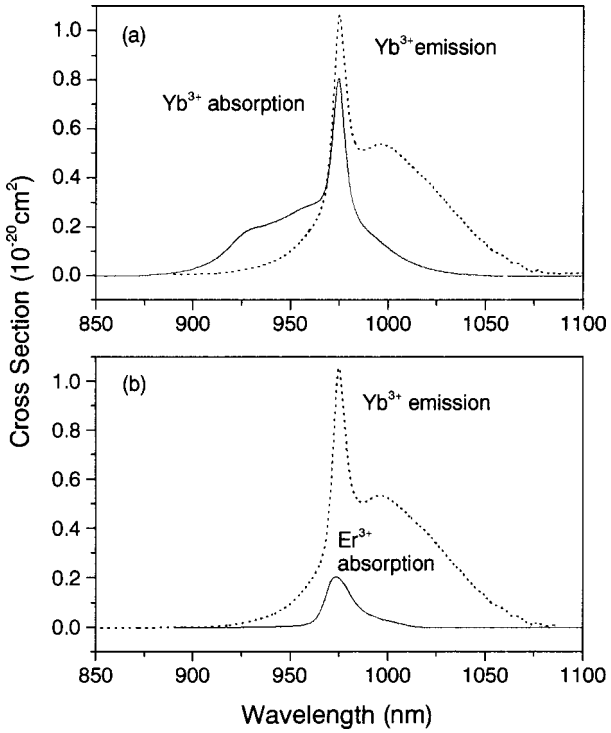

FIG. 3. Absorption (measured) and emission (calculated using McCumber) spectral cross sections for Yb^{3+} in ZBLAN (a). (b) Spectra superposition between the Yb-emission ($^2F_{7/2}\rightarrow{}^2F_{5/2}$) and the Er-absorption ($^4I_{15/2}\rightarrow{}^4I_{11/2}$) cross sections observed in Yb:Er:ZBLAN glass.

$$R_{DD}^6=\frac{6c\tau_D}{(2\pi)^4n^2}\frac{g_D^{\text{low}}}{g_D^{\text{up}}}\int\sigma_{\text{emis}}^D(\lambda)\sigma_{\text{abs}}^D(\lambda)d\lambda,$$
$$R_{DA}^6=\frac{6c\tau_D}{(2\pi)^4n^2}\frac{g_D^{\text{low}}}{g_D^{\text{up}}}\int\sigma_{\text{emis}}^D(\lambda)\sigma_{\text{abs}}^A(\lambda)d\lambda, \quad (4)$$

where c is the light speed, n the refractive index of the medium, and g_{low}^D and g_{up}^D are the degeneracy of the respective lower and upper levels of the donor. The overlap integral was calculated using the emission (D) and absorption (D or A) cross-section superposition, respectively, calculated for $D-D$, $D-A$ direct, and $A-D$ backtransfer.

The emission cross section of $Yb^{3+}(^2F_{5/2})$ was obtained from the absorption cross section spectrum using the McCumber relation[18] given by

$$\sigma_{\text{emiss}}(\lambda)=\sigma_{\text{abs}}(\lambda)\frac{N_1}{N_2}\exp\left(\frac{-\hbar\omega}{KT}\right), \quad (5)$$

where $\hbar\omega$ is the absorption photon wave number (cm^{-1}), K is the Boltzman constant, and N_1 and N_2 are the respective ground and excited state populations of donor states at the equilibrium temperature (300 K). Figure 3(a) shows the emission cross section of Yb^{3+} calculated using the population ratio $(N_1/N_2)\sim 3.04\times 10^{21}$ obtained at $T=300\,\text{K}$ using the McCumber relation (dashed curve). Figure 3(b) shows the spectral superposition between the emission cross section of Yb^{3+} and the absorption cross section of Er^{3+} obtained for ZBLAN. The strong spectral superposition observed predicts a resonant and efficient energy transfer from $Yb^{3+}(^2F_{5/2})$ to $Er^{3+}(^4I_{11/2})$ in ZBLAN. Table I shows the microscopic parameters obtained from this calculation. The fact that $C_{DD}\sim 3.8C_{DA}$ indicates that the excitation migration among Yb^{3+} ions must be an important effect in the Yb→Er energy transfer in ZBLAN glass.

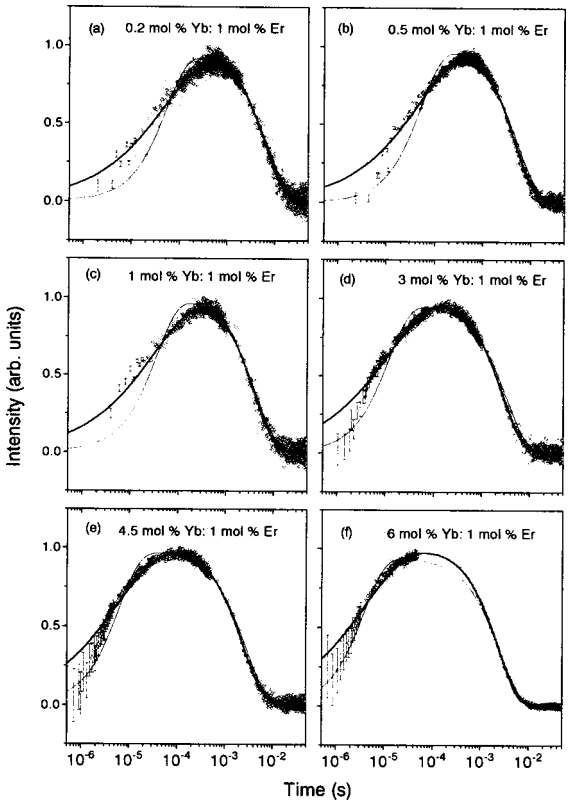

FIG. 4. Time dependence of the fluorescence of $Er(^4I_{11/2})$ at 2.7 μm measured in ZBLAN with four different Yb(x mol %):Er(1 mol %) codopings, where $x=0.2$ (a), $x=0.5$ (b), $x=1$ (c), $x=3$ (d), $x=4.5$ (e), and $x=6$ (f). The fluorescence was excited by laser pulses of 12 mJ (a)–(c), 10 mJ (d) and (f), and 7 mJ (f) (4 ns, 10 Hz) at 0.930 μm.

B. Analysis of the acceptor luminescence transient

The Yb→Er energy transfer produced the time-dependent luminescence of acceptor after the Yb^{3+} laser excitation at 0.93 μm. The time evolution of Er^{3+} luminescence at 2.7 μm was measured and analyzed using current methods found in the literature. Three sets of Yb:Er:ZBLAN glasses were produced and analyzed: (i) $(99-x)(\text{ZBLAN})\cdot x\text{YbF}_3\cdot 1\text{ErF}_3$ ($x=0.2$, 0.3, 0.5, 1, 3, 4.5, and 6); (ii) $(94-y)(\text{ZBLAN})\cdot 6\text{YbF}_3\cdot y\text{ErF}_3$ ($y=1$, 2, 3, 4, and 5); and (iii) $(99-y)(\text{ZBLAN})\cdot 1\text{YbF}_3\cdot y\text{ErF}_3$ ($y=1$, 2, 3, 4, and 5) compositions.

Figures 4(a)–4(f) exhibit the Er luminescence for the samples of set one. Figures 5(a)–5(c) and Figs. 6(a)–6(c) exhibit the luminescence results of sets two and three, respectively. Generally, we observed a nonexponential rise time of Er luminescence at 2.7 μm followed by an exponential decay with a lifetime of 2.2 ms, which is shorter than the one measured for the isolated Er^{3+} ion (~7.3 ms).

There are two possibilities to analyze the time-dependent luminescence of Er^{3+} at 2.7 μm induced by the Yb→Er energy transfer. In the first possibility, we have to solve the rate equations of the Yb–Er system considering that the do-

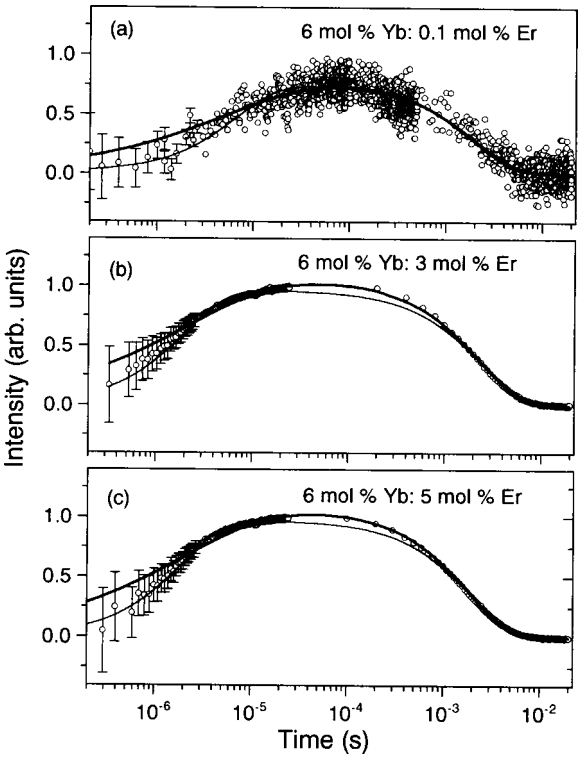

FIG. 5. Time dependence of the fluorescence decay of Er($^4I_{11/2}$) at 2.7 μm measured in ZBLAN with three different Yb(6 mol %):Er(x mol %) codopings, where $x=0.1$ (a), $x=3$ (b), and $x=5$ (c). The fluorescence were excited by laser pulses of 14 mJ (a) and (b) and 7 mJ (c) (4 ns, 10 Hz) at 0.930 μm.

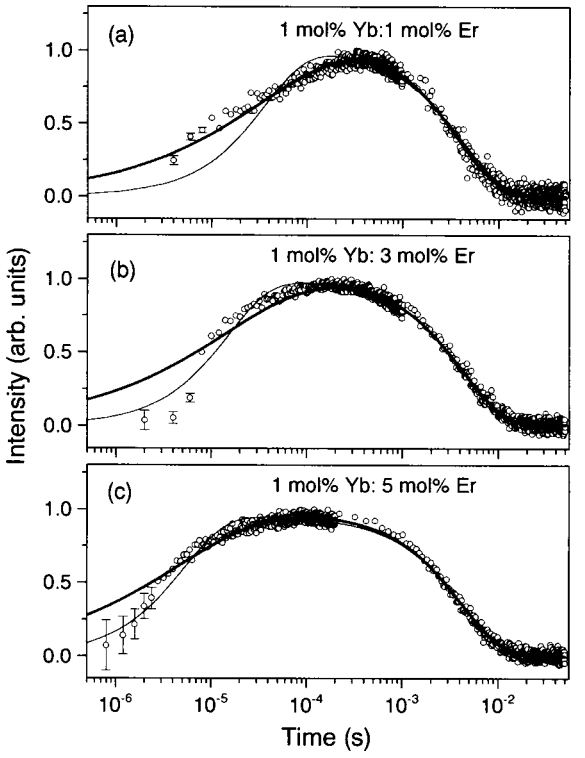

FIG. 6. Time dependence of the fluorescence decay of Er($^4I_{11/2}$) at 2.7 μm measured in ZBLAN with three different Yb(1 mol %):Er(x mol %) codopings, where $x=1$ (a), $x=3$ (b), and $x=5$ (c). The fluorescence were excited by laser pulses of 7 mJ (a) and 14 mJ (b) and (c) (4 ns, 10 Hz) at 0.930 μm.

nor (Yb^{3+}) decay time is replaced by the average of all microscopic decays, which is dependent on ($1/R^{-6}$). A simplified rate equations system is derived, in this case, if the up conversion effects on Er^{3+} luminescence are neglected. For instance, we observed that the up conversion process introduces much weaker luminescence intensities than the down conversion process. That observation is consistent with the up conversion efficiency estimated in the literature for Yb–Er in fluorides glasses[19] of $\eta_{up}\sim 6\times 10^{-2}$ considering the average power intensity of 2 W/cm^2 used in this work for Yb^{3+} excitation.

$$\frac{dn_1}{dt}=\sigma_1 I_P n_0 - k n_1 n_4 \approx n^* - k n_1$$

$$(\text{considering that } n_4 \approx 1 \quad \text{and } n^* = \text{cte}), \tag{6}$$

$$\frac{dn_2}{dt}=k n_1 n_4 - \frac{n_2}{\tau_2} \approx k n_1 - \frac{n_2}{\tau_2}, \tag{7}$$

where n_0 and n_1 are the normalized populations of the ground ($^2F_{7/2}$) and excited ($^2F_{5/2}$) states of Yb^{3+} ions. n_2 and n_4 are the populations of the $^4I_{11/2}$ and $^4I_{13/2}$ excited states of Er^{3+} ions, respectively. σ_1 is the absorption cross section of Yb^{3+} at 0.93 μm, τ_2 is the total lifetime of Er($^4I_{11/2}$), and k is the mean transfer rate of Yb→Er energy transfer. Considering a valid approximation of $n_4\approx 1$ and n^* a constant, the solution for n_2 is given by

$$n_2(t)=C\left[\exp\left(-\frac{t}{\tau_2}\right)-\exp(-kt)\right], \tag{8}$$

where C is a constant and $\tau_2=\tau_A$.

The second possibility of analyzing the 2.7 μm luminescence of Er^{3+} induced by the Yb→Er energy transfer considers that the decay rate of donor luminescence is strongly modified by the interaction with all acceptor ions included in the excitation volume. In this case, the donor and acceptor time-dependent luminescence is obtained solving the microscopic rate equation for a typical donor (D_j) or acceptor (A_k). The microscopic rate equations system is

$$\frac{d\rho_{Dj}}{dt}=-\frac{\rho_D}{\tau_D}-\sum_{i=1}^{N_A} W_{DA}(\overline{R_i}-\overline{R_j})\rho_D, \tag{9}$$

$$\frac{d\rho_{Ak}}{dt}=-\frac{\rho_A}{\tau_A}+\sum_{i=1}^{N_A} W_{DA}(\overline{R_i}-\overline{R_j})\rho_D, \tag{10}$$

where ρ_A and ρ_D are the respective probability excitation densities of acceptor (A_k) and donor ions (D_j). N_A is the number of acceptor ions in the excitation volume and $W_{DA}(R_i-R_j)$ is the microscopic energy-transfer rate. The following solutions were obtained:

$$\rho_{Dj}(t)=\exp\left(-\frac{t}{\tau_D}\right)\exp\left(-t\sum_i W_{DA}(R_i)\right), \tag{11}$$

$$\rho_{Ak}(t)=\exp\left(-\frac{t}{\tau_A}\right)-\frac{\Sigma_i W_{DA}(R_i)}{\Sigma_i W_{DA}(R_i)+\frac{1}{\tau_D}-\frac{1}{\tau_A}}$$

$$\times\exp\left(-\frac{t}{\tau_D}-t\sum_i W_{DA}(R_i)\right). \quad (12)$$

Assuming that ions A and D are randomly distributed in the glass matrix, one finds that the mean probability of donor excitation density at time t is given by the statistical average of $\rho_{Dj}(t)$ over various possible donor environments. Considering that only a dipole–dipole interaction is important, we have that the microscopic transfer rate is given by $W_{DA}=(1/\tau_D)(R_{DA}/R)^6$. In this case, the transfer rate $W_{DA}(R)$ is equal to the intrinsic decay rate $1/\tau_D$ of the donor state when $R=R_{DA}$. If the discrete lattice is approximated by a continuum in taking the averages over the interaction volume $V=(4/3)\pi R^3$ and making the limit of $V\to\infty$, one obtains the Inokuti–Hirayama[16] solution for the donor luminescence decay

$$\rho_{Dj}(t)=\exp\left(-\frac{t}{\tau_D}\right)\prod_{i=1}^{N_A}\exp[-tW_{DA}(R_i)], \quad (13)$$

$$\overline{\rho_D}(t)=\exp(-t/\tau_D)\lim_{N_A,V\to\infty}\left\{\int_V\frac{4\pi R^2}{V}\times\exp[-tW_{DA}(R)]dR\right\}^{N_A}, \quad (14)$$

$$\overline{\rho_D}(t)=\exp(-t/\tau_D)\exp\left(-\frac{C_A}{C_0}\left(\frac{\pi t}{\tau_D}\right)^{1/2}\right), \quad (15)$$

where C_A is the donor concentration and C_0 is the critical concentration given by $C_0=3/(4\pi R_{DA}^3)$. The transfer parameter was defined as $\gamma=(C_A/C_0)(\pi/\tau_D)^{1/2}$ that is also related to the microscopic transfer constant $\gamma(\text{theor})=(4\pi^{3/2}/3)C_A(C_{DA})^{1/2}$. Using the following approximation $\Sigma_i W_{DA}(R)\gg(1/\tau_D-1/\tau_A)$ in Eq. (12) and the donor luminescence solution given in Eq. (15) we obtained the time-dependent luminescence solution of the acceptor ion. This solution represents the average luminescence transient of the acceptor following the Inokuti–Hirayama approach given by

$$\overline{\rho_A}(t)=C\left[\exp\left(-\frac{t}{\tau_A}\right)-\exp\left(-\gamma\sqrt{t}-\frac{t}{\tau_D}\right)\right], \quad (16)$$

where γ is the fitting parameter which is obtained from the best fit of the time-dependent acceptor luminescence. Of course, the energy transfer in this stage does not involve the energy migration among donors. In this case, the transfer rate is equal to $\gamma^2(\text{exp})$. The solution expressed by Eq. (15) was already obtained by Inokuti–Hirayama,[16] however, the solution given by Eq. (16) was derived here and is one contribution of this present work. Many cases of resonant energy transfer between triply ionized rare earth ions are better analyzed using the acceptor luminescence transient as a probe for luminescence investigation. For instance, Tm→Ho and Yb→Er energy transfers are better analyzed measuring the 2 μm emission of $Ho^{3+}(^5I_6)$ and 2.7 μm emission of $Er^{3+}(^4I_{11/2})$, instead of monitoring the donor (Tm^{3+} or Yb^{3+}) fluorescence decay, which is almost quenched. On the other hand, the acceptor luminescence is favored by the energy transfer process and should be sufficiently intense to allow a precise luminescence measurement in a short time scale of few microseconds.

The best fits of the 2.7 μm luminescence of Er^{3+} obtained after laser excitation at 0.93 μm (Yb^{3+}) are shown in Figs. 4–6 for the three sets of sample compositions used in this work. The thick solid lines of Figs. 4–6 were used to represent the best fittings obtained using the solution given by Eq. (16) and thin solid lines represent the best fittings obtained using Eq. (8). As a general result, the time-dependent luminescence of the acceptor is better described by the solution given by Eq. (16). The acceptor luminescence involves the Inokuti–Hirayama approach instead of the solution derived from the rate equations model given by Eq. (8). In spite of this, the result shows that the best fitting value of the γ parameter is always higher than the predicted value of γ from the diffusion model. Table II shows the best fitting parameters (γ and τ_A) obtained using Eq. (16) for the case of $Er^{3+}(^4I_{11/2})$ luminescence. The predicted values of γ from the diffusion model were also included in Table II for the comparison with experimental values, $\gamma(\text{exp})$. The experimental transfer rate, $\gamma^2(\text{exp})$, and the predicted transfer rate from diffusion model, K_d, were also listed in Table II to emphasize the differences. This result indicates the existence of fast exciton diffusion among Yb^{3+} ions before starting the Yb→Er direct energy transfer. The K_d transfer rate was calculated using the following expression well known for the donor to acceptor energy transfer assisted by excitation migration among donor ions (or diffusion model): $K_d=21c_Ac_D(C_{DD}^3C_{DA})^{1/4}$.[20] It is important to note that $\gamma(\text{exp})$ values are always higher than $\gamma(\text{theor})$ values and $\gamma^2(\text{exp})$ is higher than K_d. Also we observed that the measured lifetime of the $Er^{3+}(^4I_{11/2})$ state in codoped samples is shorter (2.4–5.4 ms) than the measured lifetime of the isolated $Er^{3+}(^4I_{11/2})$ ion (~7 ms). We verify also that this luminescence lifetime difference enhances with the Yb concentration increasing for codoped samples. This lifetime effect observed in the $Er^{3+}(^4I_{11/2})$ state suggests that the Yb^{3+} ions located nearby the Er^{3+} ion increases the electron–phonon coupling enhancing its multiphonon decay rate and consequently decreasing the lifetime of the $^4I_{11/2}\to{}^4I_{13/2}$ transition.

IV. DISCUSSION AND CONCLUSIONS

The results of the investigation of Er luminescence at 2.7 μm showed that the Yb→Er energy transfer is dominated by the acceptor luminescence solution according to the Inokuti–Hirayama model, however, with the transfer parameter γ larger than that predicted by theory.[16] This mechanism was observed valid for all codoped samples used in this work (three sample sets). This physical effect is consistent with the assumption of the existence of fast excitation diffusion, which modifies the excitation distribution among donor and acceptor ions induced after laser excitation. This fast excitation diffusion occurs in a short time ($t\ll\gamma^{-2}$) leading to donor excitation approximates to the acceptor ion. Subse-

TABLE II. The experimental values of γ parameters obtained from best fit using Eq. (16) derived from the fast exciton diffusion and Inokuti–Hirayama type energy-transfer for three sets of Yb(x):Er(y):ZBLAN compositions. Theoretic values of γ parameters and K_d were obtained from the microscopic theory of energy transfer based on the random walk problem involving excitation migration by diffusion through donors states (diffusion model).

Yb:Er:ZBLAN (mol %)		Transfer parameter ($s^{-1/2}$)		$\gamma^2(10^3\ s^{-1})$	$K_d(10^3\ s^{-1})$	τ_A (ms)	$k(10^3\ s^{-1})$
(x)	(y)	γ(theor)[a]	γ(exp)[b]	(exp)[a]	(theor)[c]	(exp)[b]	(exp)[d]
0.2	1	54.8	127.0±1.9	16.1	0.7	6.07±0.09	17.6±0.4
0.3	1	54.8	128.7±1.3	16.6	1.0	5.41±0.05	18.2±0.3
0.5	1	54.8	124.4±1.2	15.5	1.6	4.43±0.04	18.6±0.3
1	1	54.8	160.4±2.9	25.7	3.3	3.80±0.06	27.1±0.7
3	1	54.8	277.6±3.2	77.1	9.8	2.71±0.04	82.2±1.5
4.5	1	54.8	407.2±3.9	165.8	14.7	2.44±0.03	156.3±2.2
6	1	54.8	484.9±5.6	235.1	19.7	2.37±0.02	256.0±3.1
1	2	113.7	246.8±3.9	60.9	6.8	4.56±0.05	58.8±1.6
1	3	171.0	285.9±5.2	81.7	10.2	4.28±0.05	64.6±1.4
1	4	229.6	416.9±4.9	173.8	13.7	4.24±0.03	147.4±3.1
1	5	283.6	464.8±6.3	216.0	16.9	4.18±0.05	182.1±3.3
6	0.1	5.7	437.1±18.3	191.1	2.1	1.90±0.09	148.3±7.1
6	0.2	11.4	409.1±8.5	167.4	4.1	2.35±0.06	148.9±3.8
6	2	113.7	564.1±6.3	318.2	40.8	2.39±0.02	305.0±2.9
6	3	171.0	692.6±6.2	479.7	61.4	2.30±0.02	496.0±4.5
6	4	229.6	670.6±8.5	449.7	82.5	2.13±0.02	480.1±3.5
6	5	283.6	695.1±8.6	483.2	101.9	1.81±0.02	494.3±3.6

[a]Calculated values using the Inokuti–Hirayama theory (Ref. 16).
[b]Experimental data obtained from best fit of the acceptor luminescence transient obtained using the Inokuti–Hirayama approach, Eq. (16).
[c]Calculated values using the diffusion model (Ref. 20).
[d]Experimental data obtained from best fit of the acceptor luminescence solution of rate equations given by Eq. (8).[a,c] Deviation estimation of these calculated parameters was 10% considering the propagation error in the absorption measurements.

quently, the Yb→Er energy transfer takes over leading the Er luminescence to exhibit a rising curve dominated by $e^{-\gamma\sqrt{t}}$. This proposed model is consistent with the observation that $\gamma(\text{exp}) \gg \gamma(\text{theor})$ and $\gamma^2(\text{exp}) > K_d$. There are two cases of $D \rightarrow A$ energy transfer (ET) considering the excitation migration. In the first, ET(1) is composed by fast diffusion among donors followed by the direct energy transfer. In the second, ET(2) is due to a diffusion assisted energy transfer. The transfer rate of ET(1) is $\gamma^2(\text{exp})$ and $\gamma^2(\text{theor}) + K_d$ is the transfer rate of ET(2). The efficiency of ET(1) was calculated considering the competition between ET(1) and ET(2) processes given

$$\text{eff}(1) = \frac{\gamma(\text{exp})^2}{\gamma(\text{exp})^2 + \gamma(\text{theor})^2 + K_d}. \tag{17}$$

Figure 7(a) shows the calculated efficiency of ET(1) as a function of Yb concentration (0.1–6) mol % of codoped samples having 1 mol % of Er^{3+}. Figure 7(a) shows that ET(1) always dominates the $D \rightarrow A$ energy transfer. It efficiency is ~0.74 for small Yb concentration (<1 mol %) and saturates near 0.95 for larger concentration (>10 mol %). Figure 7(b) shows the ET(1) efficiency dependence on Er concentration for two cases of Yb codoped samples with 1 and 6 mol %. The result of Fig. 7(b) indicates that the fast excitation (or exciton) diffusion is limited by some critical acceptor concentration. Assuming a random distribution between donor and acceptor ions in the ZBLAN matrix, we can calculate the fraction of donor (or acceptor) ions that has another neighbor donor (or acceptor) placed at the distance between R and $R + dR$ using that

$$f_i(R)dR = \frac{4\pi R^2}{R_0^3}(1 - n_i)^{4\pi R^3/3R_0^3 - 2} dR, \tag{18}$$

where $i = 1$ is used for donor–donor distribution and $i = 2$ for donor–acceptor distribution. R_0^3 is the mean volume of a hypothetic ion in glass matrix and n_i is the donor (or acceptor) concentration in molar fraction. The most simple way to calculate the efficiency of ET(1) consists of assuming the existence of a critical distance R_{C_1} between donors for the exciton diffusion efficiency and the critical distance R_{C_2} between donor–acceptor for the exciton scattering efficiency. Let us assume that the fast exciton diffusion mechanism has $\eta_{\text{diffusion}} = 1$ for donors separated by the distance $R \leqslant R_{C_1}$ and $\eta_{\text{diffusion}} = \eta_0$ for those having $R > R_{C_1}$. Second, the exciton scattering mechanism has $\eta_{\text{scatter}} = 1$ for donors having an acceptor ion at the distance $R \leqslant R_{C_2}$ and $\eta_{\text{scatter}} = 0$ if $R > R_{C_2}$. The mean efficiency of fast exciton diffusion without scattering effects is given by

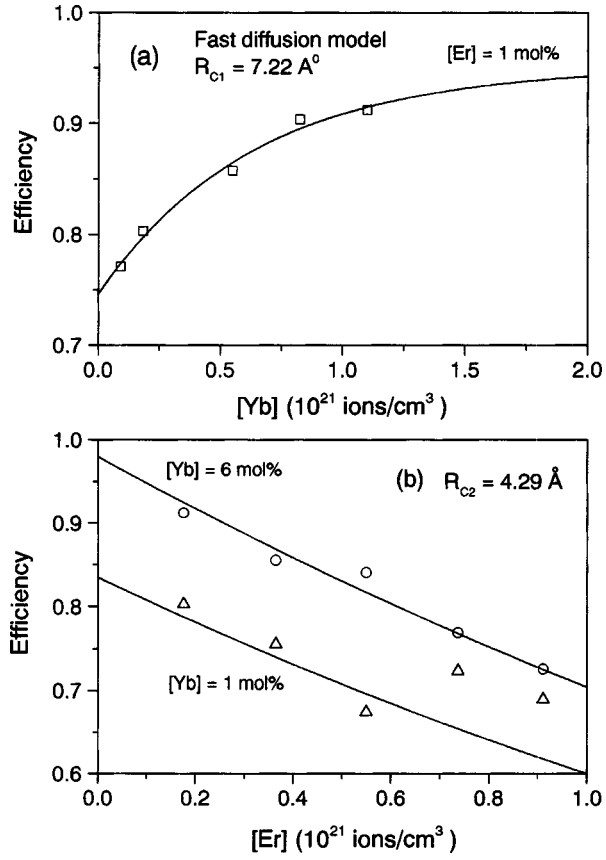

FIG. 7. The calculated efficiency of the ET(1) process as a function of Yb concentration is represented by square symbols in (a) and the solid line is the best fitting using Eq. (21). The circles and triangles are representing the calculated values of ET(1) as a function of [Er] concentration and solid lines are the best fitting using Eq. (22). The critical radii involved in the fast exciton diffusion are indicated.

$$\overline{\eta}_{\text{diffusion}} = 1\int_0^{R_{C_1}} f_1(R)dR + \eta_0 \int_{R_{C_1}}^{\infty} f_1(R)dR$$

$$= 1-(1-\eta_0)\exp\left(-\frac{4\pi}{3}R_{C_1}^3 N_D\right), \tag{19}$$

$$\overline{\eta}_{\text{scatter}} = 1\int_0^{R_{C_2}} f_2(R)dR + 0\int_{R_{C_2}}^{\infty} f_2(R)dR$$

$$= 1-\exp\left(-\frac{4\pi}{3}R_{C_2}^3 N_A\right), \tag{20}$$

where N_D and N_A are the donor (Yb) and acceptor (Er) concentrations in ions/cm^3. The total efficiency of exciton diffusion mechanism in ET(1) was obtained using that $\eta = \overline{\eta}_{\text{diffusion}}(1-\eta_{\text{scatter}})$ and the distribution function given by Eq. (18). Two expressions for the exciton diffusion efficiency were obtained: Eq. (21) for Yb concentration dependence and Eq. (22) for Er dependence.

$$\eta = 1 - a\exp\left(-\frac{N_D}{N_{C_1}}\right), \tag{21}$$

$$\eta = b\exp\left(-\frac{N_A}{N_{C_2}}\right), \tag{22}$$

a, b, N_{C_1}, and N_{C_2} are the fitting parameters (N_{C_1} and N_{C_2} are the critical concentrations related to the critical distances). a and b were also calculated from the critical concentrations (or critical radii). Figures 7(a) and 7(b) show the efficiency of the ET(1) process calculated from Eq. (17). Figure 7(a) exhibits the Yb concentration dependence and Fig. 7(b), the Er concentration dependence. Best fitting of ET(1) efficiency behavior exhibited in Figs. 7(a) and 7(b) was obtained, respectively, from Eqs. (21) and (22) (solid lines). A critical distance (R_{C_1}) of 7.22 Å was obtained giving the critical concentration of 6.34×10^{20} Yb^{3+} ions/cm^3. In addition, a critical concentration of 3.0×10^{21} Er^{3+} ions/cm^3 [or the critical radius (R_{C_2}) of 4.29 Å] was obtained from best fitting of Fig. 7(b). The respective values 0.87 and 0.98 were obtained for the b parameter using Eq. (22), for the two sets of sample compositions: $Yb^{3+}(1\%)$:Er(x%) and Yb(6%):Er(x%). Similar values of the b parameter were estimated from the critical concentration of Yb^{3+} (0.84 and 0.96, respectively). η_0 of 0.78 was estimated using the a parameter value which is consistent with our experimental observation that ET(1) dominates the Yb→Er energy transfer in ZBLAN at least for the maximum concentration investigated in this work (1×10^{21} Er^{3+} ions/cm^3).

Our main conclusion is that the fast excitation diffusion occurs in a very short time changing the initial excitation distribution among Yb^{3+} ions strongly affecting the mechanism of the Yb–Er energy transfer. The measured time dependence of acceptor luminescence is compatible with an energy transfer mechanism given in the Inokuti–Hirayama approach not involving excitation migration. However, the experimental value of the γ parameter is always larger than the expected values.[16] In spite of this, the fast exciton diffusion always dominates the excitation migration despite the (Yb:Er) composition. The method of analyzing the acceptor luminescence employed in this work constitutes an important tool to investigate the mechanism of resonant energy transfer among triply ionized rare earth ions in solids, and can be applied to other solid materials, as crystals. It is important to mention that the fast diffusion effects observed for Yb–Er energy transfer in ZBLAN may be present in any other resonant $D\rightarrow A$ energy transfer with a microscopic donor–donor transfer constant $C_{DD}\geqslant 6.8\times10^{-39}$ cm^6/s. The Tm($^3F_4$) →Ho($^5I_7$) energy transfer in YLF crystal which has $C_{DD} = 12.4\times10^{-39}$ cm^6/s,[21] could be a good candidate to apply this model to investigate the time evolution of the Ho($^5I_7$) luminescence at 2 μm after a short time laser excitation of the Tm($^3F_4$) state.

ACKNOWLEDGMENTS

The authors thank the financial support from FAPESP (Grants No. 1995/4166-0 and No. 2000/10986-0) and CNPq. One of the authors (L. D. da V.) thanks FAPESP for the fellowship (No. 2000/06798-4).

[1] M. G. Drexhage, in *Treatise on Materials Science and Technology* (Academic, New York, 1985), Vol. 26.
[2] J. Lucas, M. Chanhanasinh, M. Poulain, P. Brun, and M. J. Weber, J. Non-Cryst. Solids **27**, 273 (1978).

[3] R. Reisfeld, R. Greenberg, R. N. Brown, M. G. Drexhage, and C. K. Jorgensen, Chem. Phys. Lett. **95**, 91 (1983).
[4] R. Reisfeld, G. Katz, N. Spector, C. K. Jorgensen, C. Jacobini, and R. DePape, J. Solid Chem. Phys. Lett. **41**, 253 (1982).
[5] K. Tanimura, M. D. Shinn, W. A. Silbley, M. G. Dexhage, and R. N. Brown, Phys. Rev. B **30**, 2429 (1984).
[6] L. Wetenkamp, G. F. West, and H. Többen, J. Non-Cryst. Solids **140**, 35 (1992).
[7] S. F. Carter, M. W. Moore, D. Szebesta, J. R. Williams, D. Ranson, and P. W. France, Electron. Lett. **26**, 2116 (1990).
[8] Y. Miajima, T. Sugawa, and Y. Fukasaku, Electron. Lett. **27**, 1706 (1991).
[9] D. Ronarch, M. Guibert, H. Ibrahim, M. Monerie, H. Poignant, and A. Tromeur, Electron. Lett. **27**, 908 (1991).
[10] M. Ohashi and K. Shiraki, Electron. Lett. **27**, 2143 (1991).
[11] M. Kwasny, Z. Mierczyk, R. Stepien, and K. Jedrzejewski, J. Alloys Compd. **300–301**, 341 (2000).
[12] R. Reisfeld, M. Eyal, E. Greenberg, and C. K. Jorgensen, Chem. Phys. Lett. **118**, 25 (1985).
[13] H. M. Percival, D. Szebesta, S. T. Davey, N. A. Swain, and T. A. King, Electron. Lett. **28**, 2231 (1992).
[14] R. S. Quimby, M. G. Drexhage, and M. J. Suscavage, Electron. Lett. **23**, 32 (1987).
[15] L. Zhang, H. Hu, C. Qi, and F. Lin, Opt. Mater. **17**, 371 (2001).
[16] M. Inokuti and F. Hirayama, J. Chem. Phys. **43**, 1978 (1965).
[17] D. C. Yen, W. A. Sibley, M. Suscavage, and G. Drexhage, J. Appl. Phys. **62**, 266 (1987).
[18] D. E. McCumber, Phys. Rev. **136**, A954 (1964).
[19] D. C. Yen, W. A. Sibley, I. Schneider, R. S. Afzal, and I. Aggarwal, J. Appl. Phys. **69**, 1648 (1991).
[20] R. C. Powell, in *Physics of Solid-State Laser Materials*, edited by R. C. Powell (Springer, New York, 1998), Chap. 5.
[21] L. V. G. Tarelho, L. Gomes, and I. M. Ranieri, Phys. Rev. B **56**, 14344 (1997).